TCAD Driven CAD

A Journal for Process and Device Engineers

Accurate Simulation of Channeling Implants Using Monte Carlo Techniques

Introduction

A number of different codes have been developed for modeling implantation in crystal structures. The MARLOWE [1], UT-MARLOWE [2], and CRYSTAL-TRIM [3] codes have gained popularity and are used by many groups for studying ion implantation, sputtering and scattering from crystal surfaces. In ATHENA the current Monte Carlo models are based on PEPPER. However new models are currently implemented based on CRYSTAL, a BCA code developed at the University of Surrey, [4], which was written to explicitly meet the requirements for modeling of channeling implantation plus damage accumulation in crystalline silicon. These new models will be available in ATHENA and later in 3D in ODIN.

New Model Description

To calculate the penetration and depth distribution of bombarding particles, the model uses the well-known Binary Collision Approximation (BCA), in which, the deflection of the trajectories of moving particles is calculated in a strict binary way - between the moving atom and the closest atom in the lattice. The code has been developed extensively in two aspects: i) to account for changes in the target structure due to the ion bombardment and, ii) to account for ion implantation through two and three dimensional topography at the surface. Since the principles of BCA simulation have been described elsewhere [5] (and references therein), we will only briefly note the details here.

The ion implantation is simulated by following the fate of a large number of sequentially generated pseudo-projectiles, each of which carries an equivalent dose corresponding to a fluence increment obtained by dividing the total fluence by the number of pseudo-projectiles and scaled for the topography of interest.

After the collision cascade has been completed (i.e. the energies of all moving particles have dropped below some predetermined cut-off values), the probability $\mathcal{P}$ for each grid point is calculated, the average value of which is proportional to the damage buildup. In the subsequent collision cascade the choice of partner for interaction depends on the value of $\mathcal{P}$. $\mathcal{P}$=1 represents undamaged, perfect crystal.

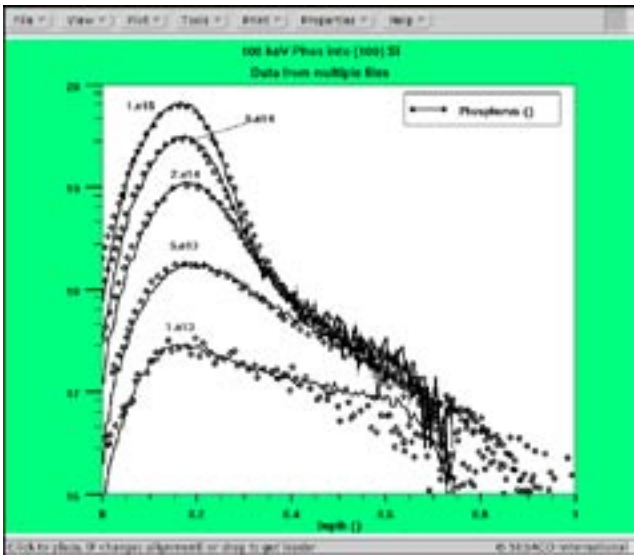

Figure 1. Phosphorus depth profiles for implantations at 100 KeV in <100> direction. The experimental profiles are collected from [10] (experiments were performed with VARIAN/EXTRON 220 implanter, 'well channeled' conditions were maintained across the wafer by comparing SIMS depth profiles from different spots). The simulation is with 0^{o} tilt, 0.5^{o} beam divergence and 16 Å surface oxide layer. Different curves represent different fluences in the range of 10^{13} cm^{-2} to $10^{15}cm^{-2}$.

The atomic collisions are considered to be composed of a quasi elastic part and of an essentially separate electron excitation part. The barycentric scattering angle is evaluated with the MAGIC formula, [6]. The present program uses the screened Coulomb potential with the universal screening function described in [6]. In order to simulate the channeling, the model uses non-local and local inelastic energy models. The local, i.e.

Continued on page 2....

INSIDE

SILVACO International

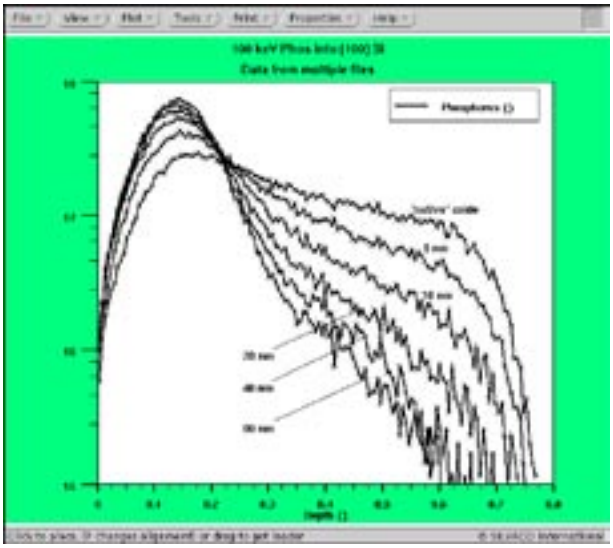

Figure 2. Surface oxide thickness dependence of Phosphorus depth profiles. Simulation conditions as in Figure 1, the ion dose for all profiles is 10^{13} cm^{-2}. Currently the SVDP models do not include screen oxide dependence for Phosphorus. This model will be used to extend the SVDP tables in the absence of experimental data.

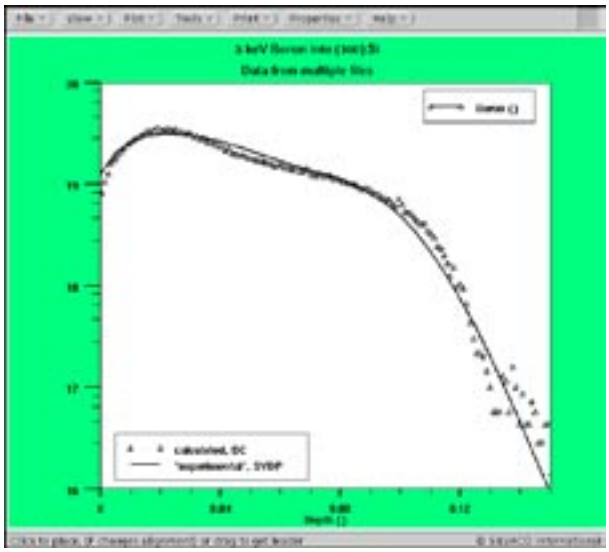

Figure 3. Low energy (5 Kev) Boron implant into crystalline silicon. The calculated profile is compared with Sims Validated Dual Pearson model [11] available in ATHENA. The simulation conditions are 0^{o} tilt and 10Å screening oxide layer.

impact dependent inelastic energy loss model is either Firsov's 5^{th} power. [7], or Oen-Robinson's exponential model, [8]. Usually, for metals, a small amount of non-local energy loss is needed in order to approximate the electronic density in the middle of the channels. At present, our model uses the same inelastic model for silicon, although the picture there might be quite different for light ions and/or high energies where valence electrons play the primary role in inelastic energy losses.

To be able to make direct comparisons to the experiments, the model takes into account damage accumulation with the ion dose. The amount of damage, at the end of each cascade, recurrently depends on the previous one and the current density of newly created disorder.

The model is highly embedded into ATHENA, allowing for modeling of ion implantation through two dimensional surface structures and the possibility of performing ion implantation in targets with any initial surface topography. Also, re-implantation due to scattering from different surface planes any number of inclusions with different structure and density are automatically taken into account.

Examples

Careful examination of all available experimental data shows big discrepancies in depth profiles among different research groups. The main differences are due to three main factors:

i) implantation geometry (beam divergence,beam alignment along crystallographic channels) and proper control to maintain it,

ii) the quality of the target surface,

iii) the depth profile measurements.

Any kind of consolidation between experiment and simulation should take into account these factors (a good example of how the misalignment with the channel changes the profiles is given in [9]). Therefore we have selected published experiments with estimated misalignment, beam divergence and quality of the surface.

The figures are for simulation of ion implantation under channeling conditions. This is a challenging problem since channeled profiles are very sensitive to the electronic energy losses and the damage model, and any discrepancy between simulation and experiment indicates the inapplicability of the inelastic loss or damage models chosen. The choice of surface orientation, angle of bombardment and beam divergence depends on the setup in the available experimental data. Universal screening function, Oen-Robinson model local energy loss and dynamic accumulation of the damage were used throughout the simulations.

References

[1] M.T. Robinson and I.M. Torrens. Physical Review B, Vol.9, pp.5008—5024, 1974.

[2] S.J. Morris, B. Obradovic, S.-H. Yang, and A.F. Tasch. IEDM Technical Digest 1996

[3] M. Posselt. Radiation Effects and Defects in Solids, Vol.130—131, pp.87—119, 1994.

[4] I. Chakarov and R. Webb. Radiation Effects and Defects in Solids, Vol.130—131, pp.447—452, 1994.

[5] W. Moeller. Simulation of Stopping and Ranges , volume 155 of NATO ASI Series E: Applied Sciences. Kluwer Academic Publishers, Dordrecht, 1989.

[6] J.F. Ziegler, J.P. Biersack, and U. Littmark. The Stopping and Range of Ions in Solids, volume 1 of The Stopping and Ranges of Ions in Matter. Pergamon Press, Oxford, 1985.

[7] O. B. Firsov. Sov. Phys. - JETP, Vol.36, p.1076, 1959.

[8] O.S. Oen and M.T. Robinson. Nuclear Instruments and Methods , Vol.132, pp.647—653, 1976.

[9] E.H.A. Dekempeneer, P.C. Zalm, G. van Hoften, and J. Politiek. Nuclear Instruments and Methods}, Vol.B48, pp.224—230, 1990.

[10] R. J. Schreutelkamp, V. Raineri, F. W. Saris, R. E. Kaim, J. F. M. Westendorp, P. F. H. M. van der Meulen, and K. T. F. Janssen. Nuclear Instriments and Methods, Vol.B55, pp.615—619, 1991.

[11] Al F. Tasch, H. Shin, C. Park, J. Alvis and S. Novak, J. Electrochem. Soc., Vol. 136, pp 810-814, 1989.

Integration of New Physical Models in ATHENA

Introduction

As a commercial process simulator ATHENA has to combine together physical models from different research groups into a single program. ATHENA covers arbitrary customer requirements by a hierarchical set of models for the complete process flow in a fully integrated environment. Models developed by different research groups are linked together. Within ATHENA these models are subjected to rigorous conditions. They have to yield reliable results in all types of applications for arbitrary geometries. All models are combined with state of the art numerics and gridding features.

For years TCAD tools suffered from limited use through user hostile interfaces and lack of code stability. A comprehensive set of interactive tools makes ATHENA easy to use and provides common functionality in separate easy-to-maintain programs. User access to all model parameters together with the C-Interpreter environment, a common feature of all SILVACO products, guarantees a maximum extent of customization.

This article will focus on the latest deep sub-micron related developments in silicon such as defect controlled diffusion, implantation and induced defects.

Diffusion Models

The three original diffusion models (`FERMI`, `TWO.DIM`, `FULL.CPL`) are simple point defect damage models. The default, `FERMI`, assumes a constant level of point defects and therefore does not account for defect enhanced diffusion. As `TWO.DIM` solves the two-dimensional distribution of point defects and includes point defect generation during implant and oxidation, it is suitable for oxidation/ silicidation enhanced diffusion. The fully coupled model (`FULL.CPL`) takes into account coupling between point defects and individual dopants. However, it ignores reactions between defects and defect pairs. It can be used for simulation of transient diffusion phenomena, low temperature diffusion and co-diffusion of dopants (emitter push effect). Damage is described as a simple distribution of both types of defects and sealed to the implanted dopant with the "scaled +1" model.

The advanced diffusion models are made up of a) Daniel Mathiot's advanced diffusion models, `CNET`, b) Peter Griffin and Scott Crowder Advanced Diffusion Models, `SU.MOD` and c) extensions to control implant damage profiles.

a) `CNET` model is an extension to full.cpl, allowing better description at very high dopant concentrations. The main additions are: percolation model, static clustering model for Boron and Arsenic, dopant / defect pairs contribution in the total diffusivity, dopant / defect pairs involve in bimolecular point defect recombination.

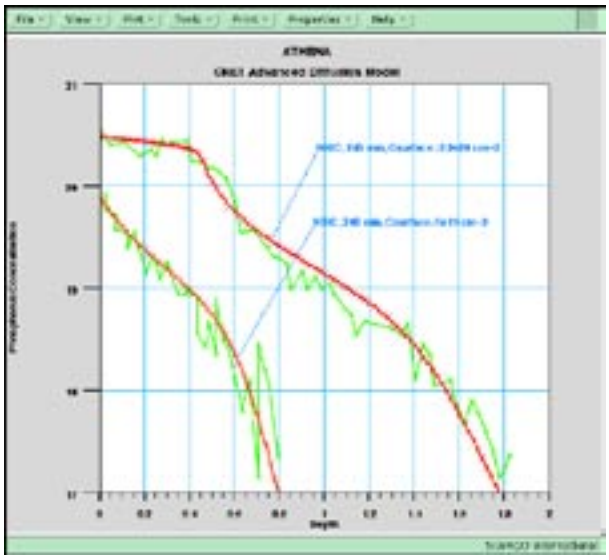

Figure 1. New pre-deposition models accurately simulate high dose effects.

b) `SU.MOD` extends `FULL.CPL` with dopant/defect interaction with other defects and with interfaces. Moreover, it allows introduction of <311>-cluster during implantation. The model suggests that the clusters dissolve in time, injecting point defects as they disappear (S. Crowder, IEDM 95, p 427). The rate of interstitials released into silicon is decaying exponentially with time, the time constant being a function of temperature. Optionally, dislocation loop interstitial sinks can be introduced. This model is a first order approximation for dislocation loop interaction with point defects. The recombination rate is proportional to the local non-equilibrium interstitial concentration.

Continued on page 11....

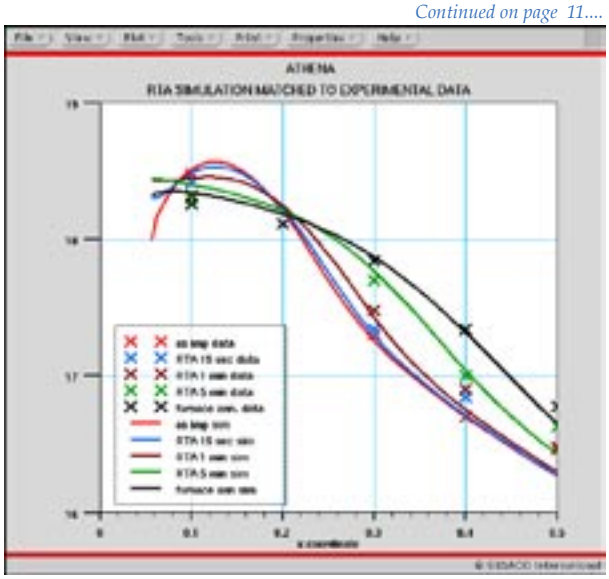

Figure 2. Improved default coefficients with the <311> cluster model provide accurate modeling.

Dopant-Dependent Oxidation Modeling in ATHENA

Introduction

The fabrication of integrated circuit microelectronic structures and devices vitally depends on the thermal oxidation process for the formation of gate dielectrics, device isolation regions, spacer regions, and ion implantation mask regions. It is well known that silicon dioxide (SiO_2) formation on highly-doped n-type and p-type substrates can be enhanced compared to SiO_2 formation on lightly-doped silicon substrates [1-6]. Of prime importance is the precise control of the oxide thickness as device geometries continue to scale to deep sub-micron dimensions. The general-purpose process simulator ATHENA includes numerical thermal oxidation models, allowing the substrate dopants influence on the oxidation kinetics to be simulated. This article is intended to review the physically-based dopant-dependent oxidation models implemented in ATHENA and to demonstrate the compatibility of thermal oxidation simulation results to measured data.

Model Description

The oxidation process is modeled by considering three steps: transport of oxidant across the ambient/SiO_2 interface, diffusion of oxidant molecules across the growing SiO_2 layer, and reaction of oxidant at the silicon/SiO_2 interface [7]. The numerical oxidation models (COMPRESS and VISCOUS) implemented in ATHENA solve the oxidant diffusion equation at incremental times steps at discrete grid points in the growing SiO_2 layer. The diffusion equation is given by

$$\frac{\partial C}{\partial t} = \vec{\nabla} \cdot \vec{F} \qquad (1)$$

where C is the oxidant concentration in SiO_2, t is the oxidation time, and F is the oxidant flux (the number of oxidant molecules crossing a unit surface area of SiO_2 in unit time). To solve equation (1), the oxidant flux needs to be specified in the growing SiO_2 layer and at material interfaces with SiO_2.

At the ambient/SiO_2 interface oxidant is transported across the interface and the corresponding flux is given by

$$\vec{F} = h\,(C^* - C_o)\,\hat{n}_{out} \qquad (2)$$

where h is the gas-phase mass transport coefficient, C* is the equilibrium oxidant concentration in SiO_2, C_0 is the oxidant concentration in SiO_2 at the ambient/SiO_2 interface, and n_{out} is a unit vector normal to the ambient/SiO_2 interface directed from silicon to SiO_2.

The diffusion of oxidant molecules in SiO_2 is driven by a concentration gradient and is expressed as

$$\vec{F} = -D\nabla C \qquad (3)$$

where D is the oxidant diffusivity in the growing SiO_2 layer, and C was defined in equation (1).

At the silicon/SiO_2 interface the oxidant reacts with silicon atoms to form a new layer of SiO_2 and the corresponding flux is given by

$$\vec{F} = k_s\ C_i\ \hat{n}_{in} \qquad (4)$$

where k_s is the reaction rate constant, C_i is the oxidant concentration in SiO_2 at the silicon/SiO_2 interface, and n_{in} is a unit vector normal to the silicon/SiO_2 interface directed from SiO_2 to silicon. At other material interfaces with SiO_2 the oxidant flux is set equal to zero. Note that the equations describing volume consumption of silicon and volume expansion of SiO_2 have not been presented here. Detailed description of these equations can be found in SILVACO literature.

From equations (1-4) and considering steady-state conditions, the familiar Deal-Grove linear-parabolic growth law [7] can be derived. Silicon dioxide growth on extrinsic silicon substrates can be modeled [1] by a modification of the Deal-Grove linear-parabolic growth law. The dependence of silicon dioxide growth kinetics on doping concentration is manifested as part of the linear rate constant, where the physical significance of the high doping levels has been explained primarily as an electrical effect [1-3]. The modified linear rate constant, including the doping dependence, becomes [1]

$$\left(\frac{B}{A}\right) = \left(\frac{B}{A}\right)_i \left(\frac{B}{A}\right)_{doping} \qquad (5)$$

where $(B/A)_i$ is the linear rate constant on intrinsic silicon, and

$$\left(\frac{B}{A}\right)_{doping} = \left[1 + K\left(\frac{V}{V_i^*} - 1\right)\right] \qquad (6)$$

where V is the vacancy concentration in silicon at the silicon/SiO_2 interface, V_i^* is the equilibrium vacancy concentration in intrinsic silicon, and K is an Arrhenius experimentally-determined coefficient.

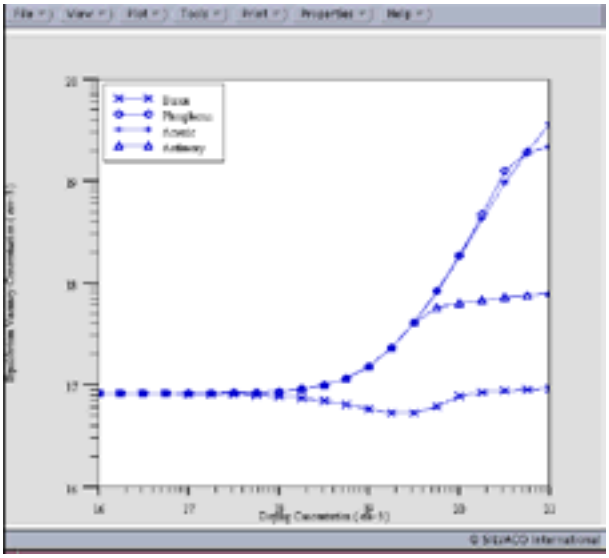

Figure 1: Equilibrium Vacancy Concentration in Silicon Versus Doping Concentration for Common Silicon Dopants at 950 ^{O}C.

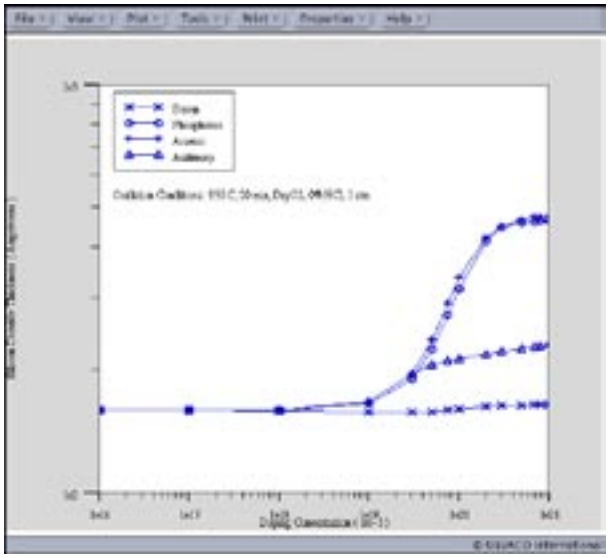

Figure 2: Simulated Silicon Dioxide Thickness Versus Doping Concentration for Common Silicon Dopants.

In general, the doping type and concentration level in the silicon substrate cause a variation in the location of the Fermi level. A shift in the Fermi level alters the equilibrium vacancy concentration in the silicon substrate [8, 9]. Figure 1 shows the functional dependence of the equilibrium vacancy concentration at 950 ^{O}C versus doping concentration for commonly used silicon dopants. The physical significance of an increase in the vacancy concentration is an increase in the number of available reaction sites for the incoming oxidant, which in turn enhances the oxidation rate.

The influence of doping concentration on SiO_2 thickness can be seen in Figure 2, where a large enhancement (with respect to the lower doping concentrations) in SiO_2 thickness is observed on highly-doped n-type substrates, and less enhancement for the p-type dopant. This trend is consistent with Figure 1, where the equilibrium vacancy concentration at high doping levels is larger for the n-type dopants than the p-type dopant.

For completeness, Figures 3-6 show plots of SiO_2 thickness versus doping concentration for boron, phosphorus, arsenic, and antimony substrates respectively, with temperature as a parameter. These four figures can be used to easily make "eye-ball" predictions of the SiO_2 thickness dependence on temperature and doping concentration for the given oxidation conditions.

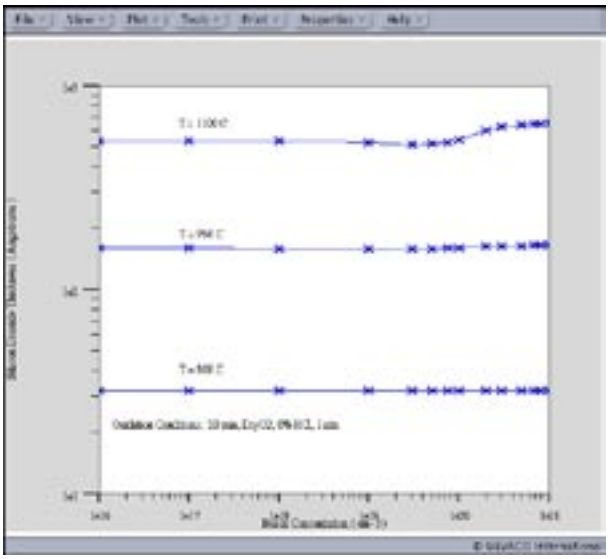

Figure 3: Simulated Silicon Dioxide Thickness Versus Boron Concentration with Temperature as a Parameter.

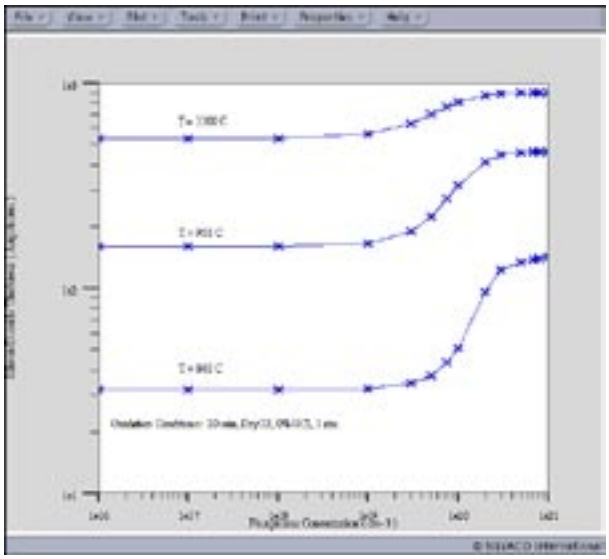

Figure 4: Simulated Silicon Dioxide Thickness Versus Phosphorus Concentration with Temperature as a Parameter.

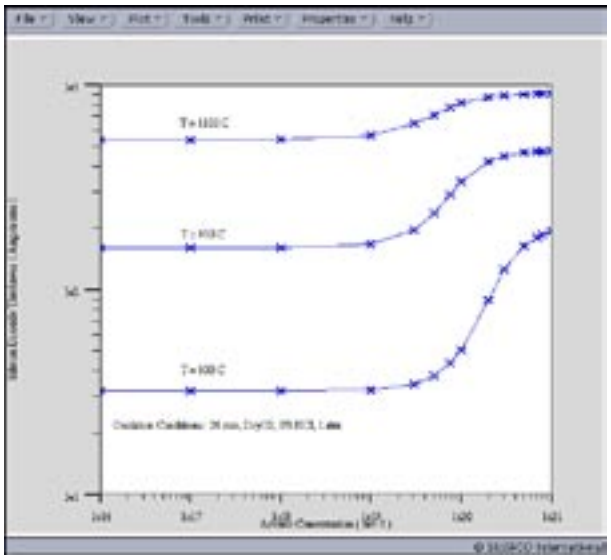

Figure 5: Simulated Silicon Dioxide Thickness Versus Arsenic Concentration with Temperature as a Parameter.

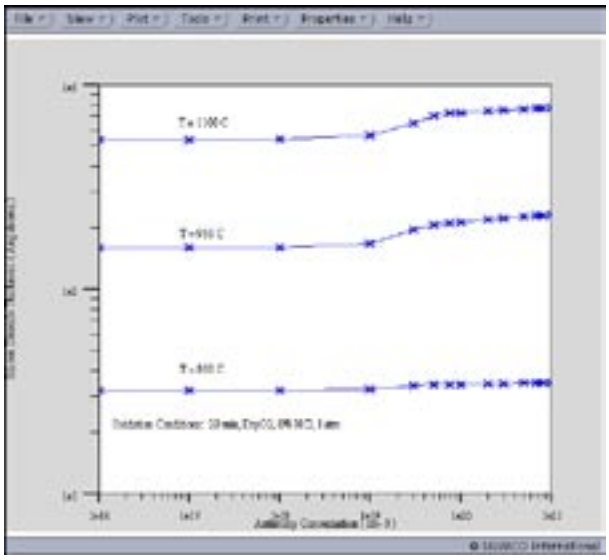

Figure 6: Simulated Silicon Dioxide Thickness Versus Antimony Concentration with Temperature as a Parameter.

Simulation and Experimental Results

A number of experiments have previously been performed in order to better understand the physics of dopant-dependent oxidation on <111> silicon [3, 4] and <100> silicon [5, 10]. In this section, results predicted by the model will be compared to measured data from oxidation experiments on <100> silicon.

Figures 7-9 show a comparison between simulated and measured [5] SiO_2 thicknesses as a function of time for three temperatures, where the substrate doping conditions were B = $1x10^{16}$ cm^{-3}, B = $6x10^{19}$ cm^{-3}, and P = $8x10^{19}$ cm^{-3}, respectively. The agreement between the simulated and measured SiO_2 thicknesses is very reasonable over the time and temperature range considered. The simulations were performed with the pre-exponential of K in equation (6) equal to one-fourth of its reported value [1]. Decreasing the value of K might be justified by considering that the original reported value was extracted from oxidation experiments on <111> silicon; whereas the simulation results in figures 7-9 are for oxidations on <100> silicon.

Figure 10 shows simulated and measured [10] SiO_2 thicknesses versus time for oxidation of heavily-doped phosphorus substrates (P = $1.8x10^{20}$ cm^{-3}) for four different temperatures (800 ^{o}C, 850 ^{o}C, 900 ^{o}C, and 950 ^{o}C). These simulations used the same coefficients as those

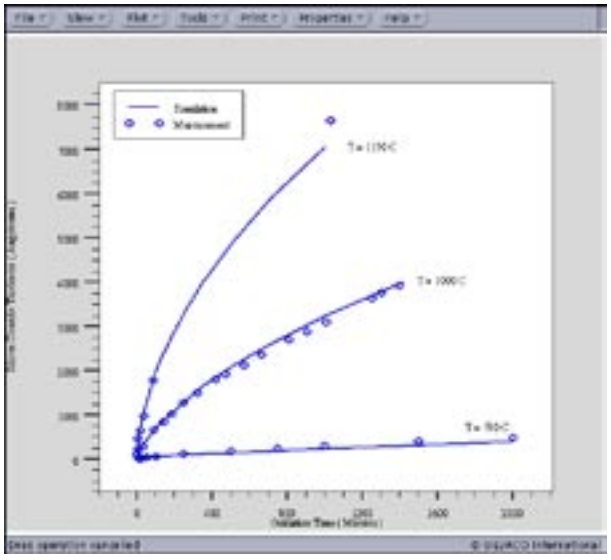

Figure 7: Comparison of Simulated and Measured Silicon Dioxide Thicknesses for Lightly-doped Boron (B = $1x10^{16}$ cm^{-3}) Substrates.

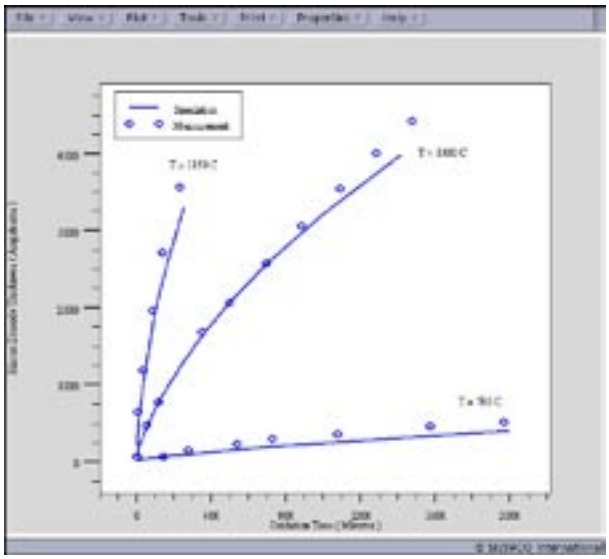

Figure 8: Comparison of Simulated and Measured Silicon Dioxide Thicknesses for Heavily-doped Boron (B = $6x10^{19}$ cm^{-3}) Substrates.

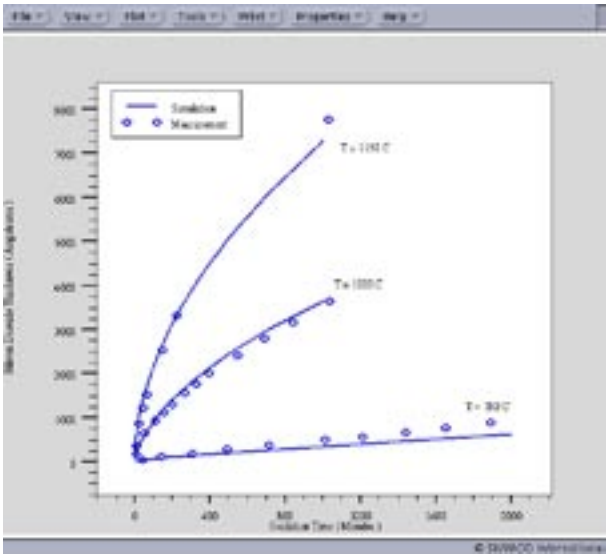

Figure 9: Comparison of Simulated and Measured Silicon Dioxide Thicknesses for Heavily-doped Phosphorus (P = $8x10^{19}$ cm^{-3}) Substrates.

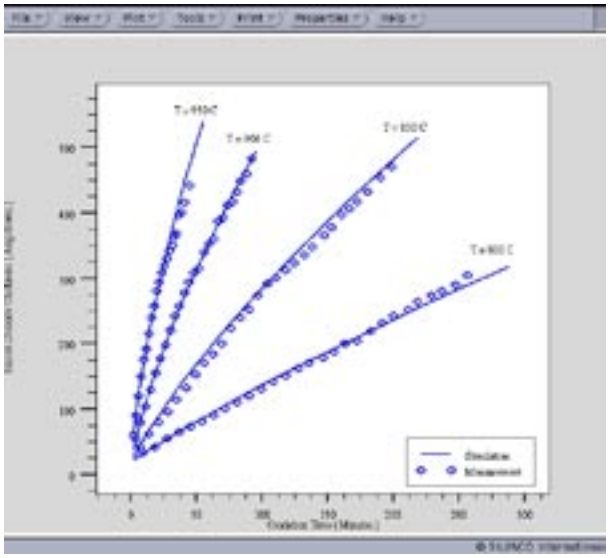

Figure 10: Comparison of Simulated and Measured Silicon Dioxide Thicknesses for Heavily-doped Phosphorus (P = $1.8x10^{20}$ cm^{-3}) Substrates.

for Figures 7-9. The agreement shown for each temperature in Figure 10 helps to justify decreasing the value of K for dopant-dependent oxidation on <100> silicon.

Conclusion

The dopant-dependent oxidation models implemented in ATHENA have been reviewed and it has been shown that the SiO_2 thicknesses predicted by the oxidation models agree reasonably with experimentally-determined SiO_2 thicknesses. It might seem feasible to decrease the value of K in equation (6) for oxidation simulations on <100> silicon because the default value of K was extracted from oxidation experiments on <111> silicon. Further, the use of simulation for silicon thermal oxidation can further aid engineers in determining process conditions for deep sub-micron devices.

Parameters Used in This Work

The tuned parameters used to match the measured data presented here will be available by default in the next release. Users of the current ATHENA release can reproduce the results by introducing the following syntax:

```
oxide silicon baf.pe = -0.46 baf.ppe = -1.0 \
       baf.ne = -0.145 baf.nne = -0.62 \
       baf.k0 = 6.5e2
```

References

[1] C. P. Ho, and J. D. Plummer, "Si/SiO_2 Interface Oxidation Kinetics: A Physical Model for the Influence of High Substrate Doping Levels, I. Theory," J. Electrochem. Soc., Vol. 126, No. 9, pp. 1516-1522, 1979.

[2] C. P. Ho, and J. D. Plummer, "Si/SiO_2 Interface Oxidation Kinetics: A Physical Model for the Influence of High Substrate Doping Levels, II. Comparison with Experiment and Discussion," J. Electrochem. Soc., Vol. 126, No. 9, pp. 1523-1530, 1979.

[3] C.P. Ho, J. D. Plummer, and J. D. Meindl, "Thermal Oxidation of Heavily Phosphorus-Doped Silicon," J. Electrochem. Soc., Vol. 125, No. 4, pp. 665-671, 1978.

[4] B.E. Deal and M. Sklar, "Thermal Oxidation of Heavily Doped Silicon," J. Electrochem. Soc., Vol. 112, No. 4, pp. 430-435, 1965.

[5] E. A. Irene and D. W. Dong, "Silicon Oxidation Studies: The Oxidation of Heavily B- and P-Doped Single Crystal Silicon," J. Electrochem. Soc., Vol. 125, No. 7, pp 1146-1151, 1978.

[6] S. M. Sze, VLSI Technology, Ch 3, McGraw-Hill, New York, 1988.

[7] B. E. Deal, and A. S. Grove, "General Relationship for the Thermal Oxidation of Silicon," J. Appl. Phys., Vol. 36, No. 12, pp. 3770-3778, 1965.

[8] W. Shockley and J. L. Moll, "Solubility of Flaws in Heavily-Doped Semiconductors," Physical Review, Vol. 119, No. 5., pp. 1480-1482, 1960.

[9] J. A. Van Vechten, and C. D. Thurmond, "Entropy of Ionization and Temperature Variation of Ionization Levels of Defects in Semiconductors," Physical Review B, Vol. 14, No. 8, pp. 3539-3550, 1976.

[10] H. Z. Massoud, "Reverse Dopant Redistribution during the Initial Stages of the Oxidation of Heavily Doped Silicon in Dry Oxygen," Appl. Phys. Lett., Vol. 53, No. 6, pp. 497-499, 1988.

Calendar of Events

August

1	
2	
3	
4	
5	
6	
7	
8	
9	
10	
11	
12	
13	
14	
15	
16	
17	ChiPPs '97, Germany
18	ChiPPs '97, Germany
19	ChiPPs '97, Germany
20	
21	
22	TCAD W/S, Japan
23	
24	
25	EUROPAR, Germany
26	
27	
28	
29	
30	
31	

September

1	
2	
3	
4	
5	
6	
7	
8	ISCS / SISPAD
9	ISCS / SISPAD
10	ISCS / SISPAD
11	
12	
13	
14	
15	RADECS '97
16	
17	
18	
19	
20	
21	
22	ESSDERC '97
23	ESSDERC '97
24	ESSDERC '97
25	
26	UTMOST W/S, Japan
27	
28	
29	BCTM - Minneapolis, MN
30	BCTM - Minneapolis, MN

Bulletin Board

Silvaco to Demonstrate Advances in Compound Material Device Simulation at ISCS 97

Silvaco will present the latest advances in compound material semiconductor simulation at the 24th International Symposium on Compound Semiconductors. The conference will be held at the Hotel Del Coronado, San Diego, CA on September 7 -11.

The recently released Quantum module allows the simulation of quantum carrier distribution by use of a Wigner function quantum moments expression that produces a quantized electron density. This can be used to accurately simulate the behavior of quantized channels and wells.

An introduction to Silvaco's innovative FastATLAS compound material simulator will be presented. FastATLAS is a comprehensive suite of device simulation models that rapidly and accurately characterizes MESFET and HEMT structures in a robust solution environment. Based on advanced algorithms, FastATLAS is several orders of magnitude faster than conventional simulation methods making it an ideal analysis and optimization tool. FastATLAS is able to extract both DC and AC behavior including s-parameters. The program includes complex physical models including a self-consistent solution of Schrodinger's equation and velocity overshoot in the hydrodynamic description of carrier transport.

Visit Silvaco at ESSDERC '97

Silvaco will be demonstrating the latest advances in physical IC simulation technology at ESSDERC '97 on September 22nd - 24th. Silvaco's engineers will be presenting demonstrations of our full line of products including; recent advances in the Virtual Wafer Fab statistical TCAD process and device simulation software tools, Silvaco's suite of process-dependent 3D interconnect parasitic extraction software, and powerful new performance enhancements and features in the SmartSpice Analog circuit simulator and industry standard UTMOST III parameter extraction and SPICE modeling software.

The conference will be held at Forum am Schloßpark, Ludwigsburg near Stuttgart. Silvaco's booth is located on the Eingangs-Foyer.

Silvaco To Address Radiation Effects at RADECS '97

Silvaco will be hosting an exhibit booth at RADECS '97, the 4th European Conference on Radiations and Their Effects on Devices and Systems. Silvaco's application engineers will demonstrate the latest in device simulation and analysis software capabilities for the modeling of the effects of radiation exposure on device performance and reliability. The conference is being held on September 15th - 19th at Cannes-Palm Beach, France.

New simulation tools to be introduced include DGEM, a module for determining reliability effects caused by defect generation, as well as a host of new capabilities for the simulation of Silicon-on-Insulator technology devices and circuits. Silvaco's experienced engineering staff will be on hand to answer questions and to demonstrate Silvaco's industry leading device simulation capabilities.

For more information on any of our workshops, please check our web site at ***http://www.silvaco.com***

Andy Strachan, Applications and Support Manager

DEVEDIT : A Flexible Tool for Structure Editing and Mesh Generation

Mesh generation has traditionally been one of the most difficult topics in the use of TCAD tools. DevEdit was released in 1992 as a structure pre-processor including interactive mesh generation. Over the previous five years significant enhancements have allowed DevEdit to become a general purpose structure editing and mesh generation tool.

An important feature of all DevEdit generated meshes is an option to not include any obtuse triangles. Obtuse triangles lead to roughness and errors in the device simulation solution. In extreme cases obtuse triangles lead to non-convergence.

The primary application of DevEdit has always been mesh generation for device simulation. Applications have fallen into three basic groups:

- remeshing of ATHENA structures before S-Pisces simulation
- pre-processing of III-V structures for Blaze
- editing of ATHENA geometries for use in ATLAS

For 3D applications, DevEdit3D is used to perform the same functions. Hints and Tips on the use of DevEdit3D for 2D to 3D interfacing are given in [1]

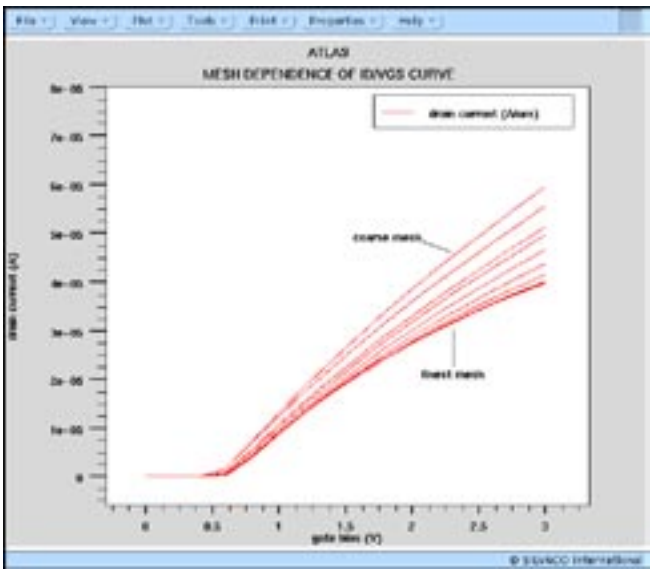

Figure 1. MOS Id/Vgs curve as function of mesh density. A finer channel mesh gives better resolution of fields and carriers which lower mobility in this case. At increasingly finer mesh spacing the results do tend to a fixed value.

Re-meshing ATHENA Structures

The grid dependence of device simulation results has been documented in several places including [2]. Results do become grid independent at certain grid spacing but this may be finer than users expect. A simple example is shown in figure 1. Unless grid density is sufficient to resolve the electric field and the carrier concentration in the channel, erroneous results may be seen. Since both electric field and carrier concentrations have steep gradients in MOS channels the surface grid spacing must generally be on the order of 0.5nm. Even the least grid sensitive modified Watt model (`MOD.WATT`) requires 5nm grid spacing which can be difficult to achieve without any remeshing.

If the structure is generated within ATLAS it is simple to create a fine surface mesh. However with structures generated by ATHENA it is generally impossible to ensure such a fine surface mesh spacing. Even if such a mesh is defined by the initial mesh generation in

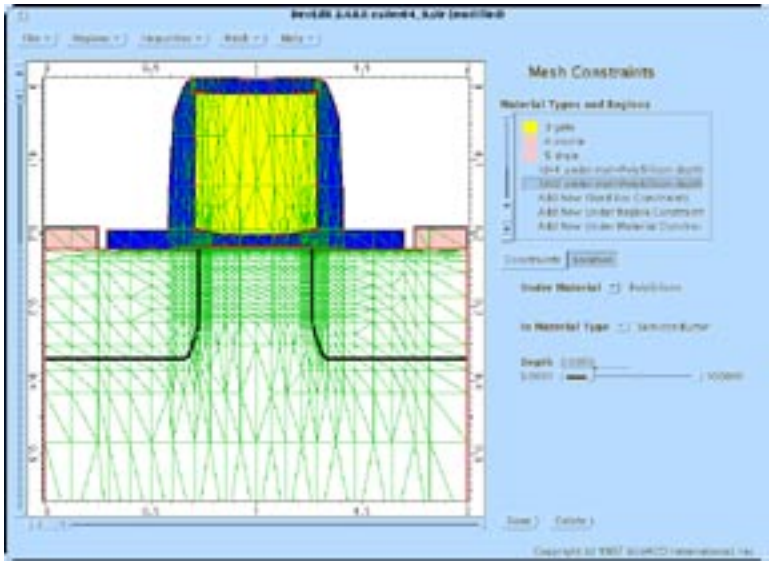

Figure 2. DEVEDIT screen illustrating a MOSFET with fine channel mesh defined using simple menu.

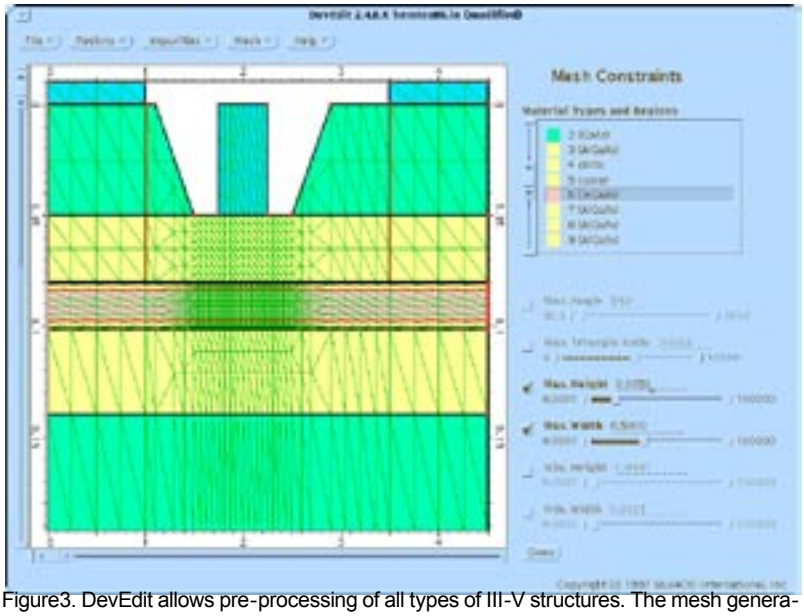

Figure3. DevEdit allows pre-processing of all types of III-V structures. The mesh generation rules allow focused mesh refinement in the channel of this measured gate HEMT.

ATHENA or by initial adaptive mesh rules the surface processing steps generally degrade the mesh. DevEdit provides a solution by allowing users to discard the mesh used in ATHENA and recreate a new mesh for ATLAS based on simple rules.

Figure 2 shows a MOSFET from ATHENA with a mesh generated by DevEdit . The menus within DevEdit allow users to specify rules for the new mesh generation. For MOS structures these rules focus on a fine mesh in the channel. For MOS it is important that the meshing rules can be made completely independent of solution quantities. Remeshing on doping or even potential gradients in the channel is usually insufficient. For bipolar devices the rules focus the mesh on the base-emitter junction. More details of this approach including syntax examples can be found in [3].

Pre-processing Structures for BLAZE

For heterojunction device simulation it is necessary to construct a structure consisting of several layers of different semiconductor materials. In many cases there is no process simulation required so ATHENA/ Flash is not appropriate. DevEdit is the easiest and most flexible program for creating III-V device structures. DevEdit allows the user to draw regions of the device interactively using the mouse. It can handle the recess profiles of HEMT or MESFET mesa structures and the stepped profiles used in HBTs. DevEdit also allows the definition of graded and abrupt heterojunctions. Following structure creation the user can mesh the structure based on the same style of meshing rules indicated above.

ATHENA Structure Editing for ATLAS

Since the CPU time required to run process simulation is super-linear with the number of grid points there can be significant CPU time savings available by splitting large simulations into sections. These sections can be joined together at the end of the process simulation using DevEdit .

Figure 4 illustrates the `JOIN` function in DevEdit allowing users to select several ATHENA structure files and join them together.

Automated Mesh Generation

Although interactive mesh generation is easy-to-use, there is a need to automate the structure editing and mesh generation process. This is done though the batch mode of DevEdit . DevEdit is implemented into DeckBuild, see Figure 5, as a fully batch mode simulator including automatic interfaces to ATHENA and ATLAS.

It is possible to construct DevEdit syntax using popup menus in DeckBuild. However the most convenient way is to use the interactive DevEdit to define the structure or mesh rules. A DevEdit command file can then be saved that includes all the commands performed in interactive mode.

These command files can be edited to allow grid definitions based on previously results of `EXTRACT` statements. This allows grids of similar structures to be formed with the same set of rules to create consistent meshes. Such an approach can be used inside the VWF automation tools to remove grid dependency when experimenting with process parameters.

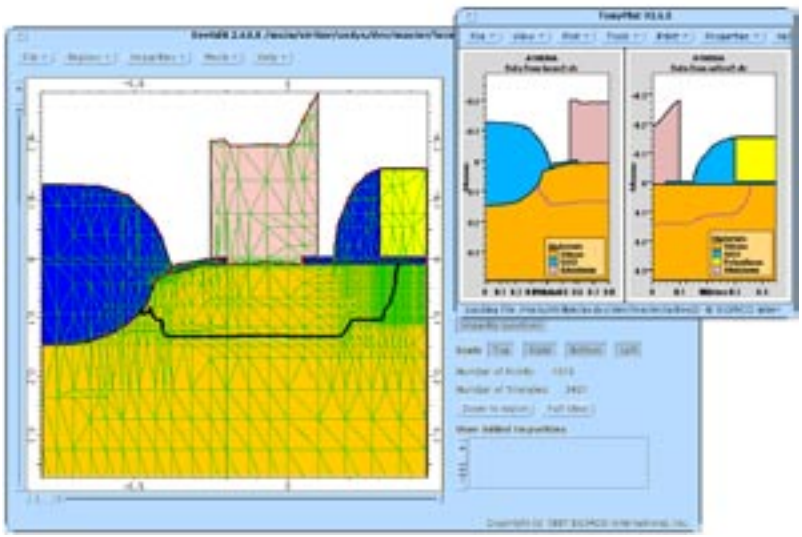

Figure 4. A single complete device structure can be constructed in DevEdit by joining two or more ATHENA results. The silicon surface is auto-aligned to leave a smooth surface.

Figure 5. DeckBuild with batchmode syntax of DevEdit. Running in batchmode allows automation of all DevEdit features.

Conclusion

Mesh generation using DevEdit allows users to create grids for arbitrary structures based on simple rules. The interactive mode makes the program easy to use while a batch mode allows automated mesh generation for similar structures. In addition to remeshing structures, DEVEDIT is used to edit structures prior to ATLAS device simulation. Features such as the `JOIN` function allow users to create large structures for device simulation from a a set of smaller process simulation results.

References

[1] Hint, Tips and Solutions, "Simulation Standard", April 1997.

[2] TCAD Calibration: Challenges and Opportunities, Michael Duane, Chipps '97 conference, (www.prismnet.com/~naomi/tcad)

[3] Hints, Tips and Solutions, "Simulation Standard", June 1996.

Call for Questions

If you have hints, tips, solutions or questions to contribute, please contact our Applications and Support Department

Phone: (408) 567-1000 Fax: (408) 496-6080

e-mail: *support@silvaco.com*

Hints, Tips and Solutions Archive

Check our our Web Page to see more details of this example plus an archive of previous Hints, Tips, and Solutions

http:://www.silvaco.com

...continued from page 3

c) The advanced diffusion models require more flexible control of implant damage generation. By setting max. and min. concentration threshold values, regions related to the implanted profile were defined for <311> clusters and dislocation loops. Similar to the scaled +1 model, clusters are distributed within these specified regions. Above the max. cluster threshold, the material is assumed to be amorphous.

Implantation Models

The ion implantation hierarchy is made up of the 2 basic model types: analytic and Monte Carlo. Universal tilt and rotation capability for both analytic and Monte Carlo calculations are available. Damage is calculated with the scaled +1 model for interstitials and also extended defects or with physical damage calculation based on energy loss in collision cascade (MC).

Dual Pearson tables based on the measurements of Al Tasch (for example A.F. Tasch et al., J. Electrochem. Soc., 136, p.810, 1989) have been implemented for a large parameter space including screen oxides. This model allows accurate simulation of channeling during implant. For implant parameter in amorphous targets, single Pearson tables are used. For multilayer targets three different correction approaches are available: dose matching (default), range matching and maximal range scaling. In 2D cases, a parabolic approximation for the depth dependence of transversal standard deviation is implemented and matched against MC results.

Outlook

New models are continually being developed by researchers around the world. Silvaco will continue to incorporate the best-available models for all process steps into ATHENA. Work is currently being done to improve low energy implantation models, introduce a more advanced stress dependent oxidation model (ISEN IEDM 1996) and improve extended defect models.

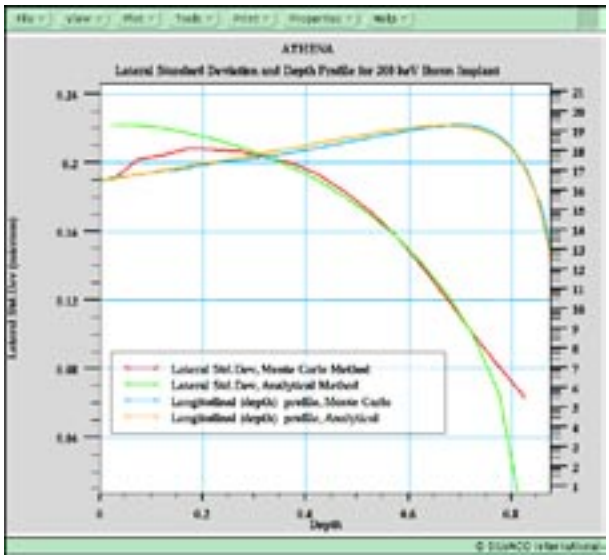

Figure 3. Integration of the latest implant research allows ATHENA to model vertical and horizontal implant profiles

SILVACO WANTS YOU!!

- SPICE Application Engineers
- Process and Device Application Engineers
- Software Developers

fax your resume to:
408-496-6080, or
e-mail to:
personnel@silvaco.com

Opportunities worldwide for apps engineers: Santa Clara, Phoenix, Austin, Boston, Tokyo, Guildford, Munich, Grenoble, Seoul, Hsinchu. Opportunities for developers at our California headquarters.

SILVACO International

4701 Patrick Henry Drive, Building 2
Santa Clara, CA 95054

Telephone: (408) 567-1000
Fax: (408) 496-6080
URL: http://www.silvaco.com